PERFORMANCE ANALYSIS OF PEDESTAL FANS AN EXPERIMENTAL INVESTIGATION

A. G. T. Sugathapala and P.B.I. Somarathne
Dept. Mechanical Engineering, University of Moratuwa.

PERFORMANCE ANALYSIS OF PEDESTAL FANS: AN EXPERIMENTAL INVESTIGATION

A. G. T. Sugathapala and P.B.I. Somarathne
Dept. Mechanical Engineering, University of Moratuwa.

ABSTRACT

Performances of pedestal fans were analysed through experimental measurements of the induced flow field (velocity distribution) and the power consumption by two different types of fans. A test rig was constructed to facilitate the measurement of axial flow velocities in the three dimensional space. In order to predict the jet pattern produced by the fan, axial velocity distributions on sufficient number of planes were measured. These data were used to calculate the jet diameter, flow rate, kinetic energy and the linear momentum of the flow at different planes from the rotor. The power consumption and the angular speed of the rotor for each regulator setting were also measured.

The velocity distributions measured on different planes from the rotor clearly illustrate the general characteristics of the flow generated by free flow fans, including the reverse flow near the rotor plane, jet entrainment and diffusion. The results show that the overall energy efficiency of a fan depends critically on its speed (i.e. regulator setting); efficiency increases with the speed. The results also indicate that the service factor defined by the flow rate at a specified section divided by the power consumption is not a suitable performance index for free-flow fans. Even with a similar axial velocity profile generated by two different fans could result in two different jet developments leading to completely different flow characteristics and performances. The results of the present study indicate the complexity of the jet development and the necessity for detailed experimental measurements of the flow velocity distribution including the swirl components in predicting performance of free-flow fans.

INTRODUCTION

Free-flow fans are commonly used in buildings to achieve the necessary thermal comfort levels. The flow generated by a fan provides the required circulation and velocity for comfort. Further, steady and uniform temperature conditions in the space could be maintained. The overall performance of a free-flow fan is determined by the aerodynamic design of the rotor blades together with the correct matching of the electric motor characteristics at different speeds (i.e. at different regulator settings). The characteristics of the air-jet generated by the fan, especially the velocity profile at the rotor plane and jet swirl, determine the extent of the comfort region in space developed by the fan. Another factor that affects the effectiveness of the fan is the presence of solid boundaries, such as walls and furniture in the vicinity of the fan rotor and the air jet. There are a number of different brands of free-flow fans available in the market with different design features (i.e. different blade shapes, sizes, number of blades etc.). In general, performance characteristics of air-circulating fans are not provided to the customer. In some cases, wide variations in the performance could be observed among the fans even with the same design and brand. These observations indicate the difficulty of drawing a general conclusion on the relative performances of different types of free-flow fans and recognize the need for performance testing of each brand and design.

Among the available types of free flow fans pedestal and table fans are the most common types used in domestic sector. Generally these design has some notable advantages such as flexibility in placing, wider coverage through rotor swing facility, etc. These fans have high solidity rotors with propeller type blades, where the chord length and blade angle vary continuously for maximum performance.

The flow field generated by a free-flow fan is very complex and difficult to predict theoretically as well as experimentally. Thus the prediction of the performance is not an easy task. Modern experimental techniques, such as laser doppler velocimetry and wide-field shadowgraphy, could be used to obtain data necessary for detailed study. However, these experimental setups are expensive and the testing is difficult to perform (Conlisk 1997). Further, theoretical methods such as free vortex techniques and three-dimensional Navier-Stokes computations are computationally intensive (see Ahmad & Duque 1996 for applications in helicopter rotors). Therefore, the only alternative available would be to have less detailed study based on experimental investigation using basic instruments. Such a method is presented in the SL Standards for fan testing (SLS 814 - Part 1), where the axial velocity distribution on a specified plane from the fan rotor is to be measured to calculate the flow rate at different regulator settings. Then the performance of the fan is evaluated by the ratio between this flow rate and the electric power consumption, which is known as service factor. Previous investigations based on testing of ceiling fans showed the limitations of the service factor as a performance index for air-circulating fans (Sugathapala 1997).

The present study is carried out to investigate further the performance of free-flow fans through testing of pedestal fans. A number of fans are tested and results of two similar fans of different brands are presented and analyzed in this paper. The measurements include jet development pattern, velocity distributions and power consumption at different regulator settings. These results too clearly show the ineffectiveness of the service factor as a performance index of free-flow fans. The present study is also aimed at introducing an alternative method for fan testing which will be more useful in selecting fan(s) for particular application.

BASIC CHARACTERISTICS OF PEDESTAL FANS

Geometric Characteristics

Pedestal fans have propeller type rotors with three blades (most common) with continuously varying chord lengths and blade angles. Blades are made out of plastic or sheet metal with a circular arc profile. Usually the rotor has high solidity (i.e. ratio of blade area to rotor area) compared with ceiling fans.

Pattern of Flow

The mechanical energy generated by the electric motor is converted into fluid energy through a hydrodynamic action of the fan rotor, in the form of flow rate through the rotor together with a pressure rise across it. As a result, the fan discharges a jet of air possessing a free boundary (see Figure 1). Since the fan is operating in a common, unrestricted space, it is fed principally by air that has returned to the inlet side of the fan by the medium of a converging stream of reverse flow outside the jet. Even in front of the rotor, the streamlines of the jet converge rapidly and become parallel within a short distance. While the surrounding air in contact with the jet is accelerated due to the transfer of momentum through the action of shear forces, and more and more air is entered to the jet. This process of entrainment continues as the air stream moves further away from the fan and the jet expands owing to the increase in flow rate. Finally, the momentum of the jet reaches zero and entrainment ceases, and there is a net loss of air through the boundaries as the kinetic energy of the jet is steadily

converted into kinetic energy of turbulence, which decays through viscous shear (see Figure 2). The buffer region between the diverging jet and the reverse flow is one of large-scale random turbulence except in the near vicinity of the fan (Wallis 1983). The rotation of the blades also imparts a swirl to the jet flow, which determines the rate of jet diffusion (Rajaratnam 1976) and therefore the amount of jet penetration.

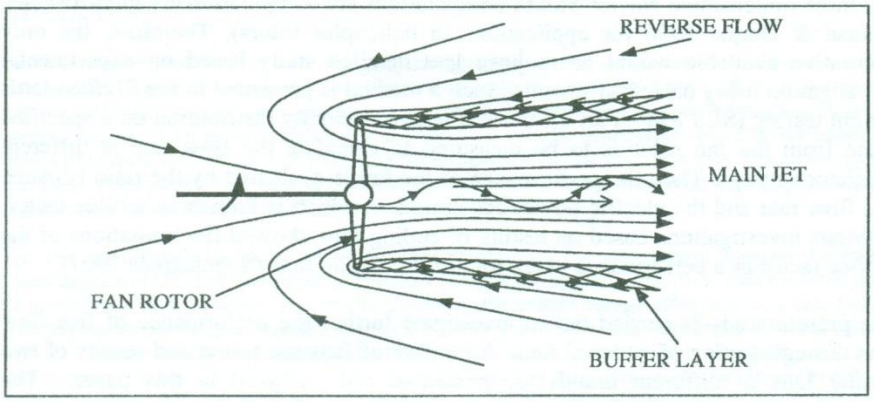

Figure 1: Pattern of flow in the near vicinity of the rotor

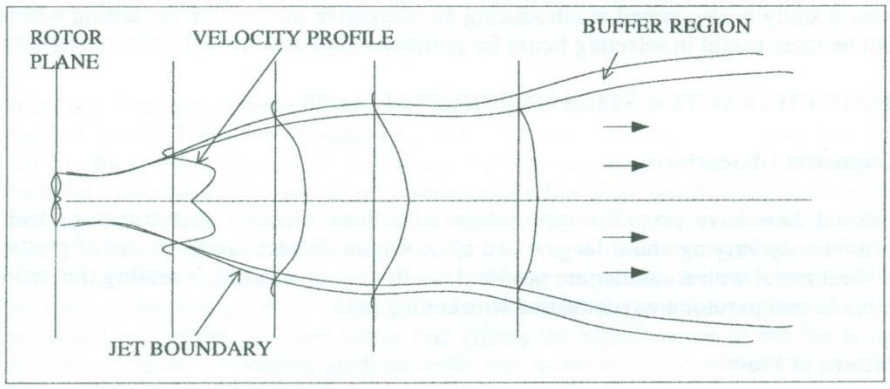

Figure 2: Jet development

EXPERIMENTAL SETUP

The air velocity was measured by using a rotating vane digital anemometer with a resolution of 0.01 m/s. It was mounted on the test grid, which has a facility to move the anemometer to any point in the three-dimensional space within the required limits, as shown in Figure 3. The energy was measured by means of digital wattmeter with a resolution of 0.5 W. The angular velocity of rotor measured by using a stroboscope.

The axial velocity distributions generated by a fan were measured on different planes from the fan along two diametrical directions, one horizontal and one vertical, and the power consumption by the fan at each case was also measured. These data were

collected at different regulator settings for two pedestal fans of same rotor size but different brands.

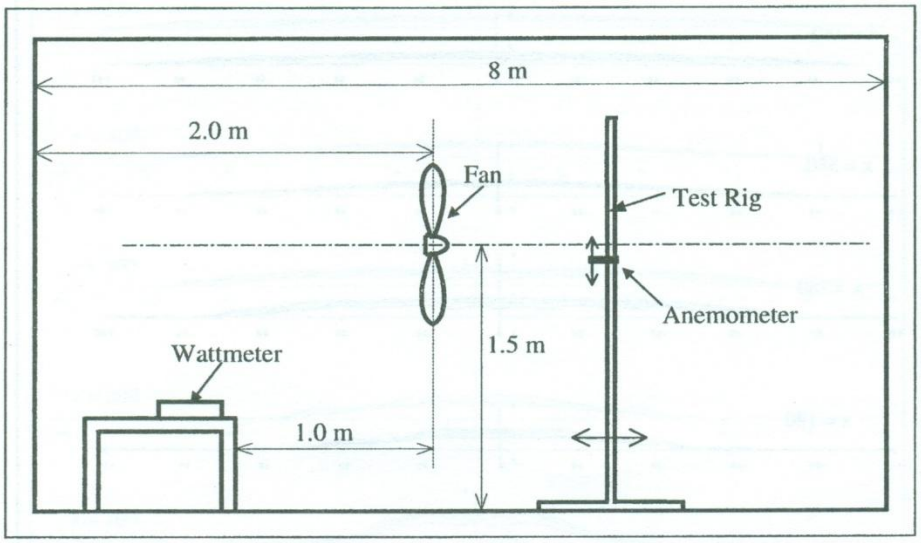

Figure 3: Experimental setup

MEASUREMENTS

The measured data for the two pedestal fans are summarized below:

Power Consumption and Rotational Speeds

Fan Model	Parameter	Regulator Position		
		1	2	3
Pedestal Fan Brand - A	Rotational Speed (rpm)	734	957	1178
	Power Consumption (W)	45	51	57
Pedestal Fan Brand - B	Rotational Speed (rpm)	877	1005	1166
	Power Consumption (W)	41	44	46

Table 1: Power consumption and rotational speeds at different regulator positions.

Velocity Distributions

Velocity distribution at one plane of the pedestal fan - A is given in the Appendix. Similar set of readings was taken for eight more planes for each regulator position. The procedure was repeated for other regulator positions for each fan. Therefore, there are altogether 54 set of such reading. These data are not provided with this paper, but presented graphically here.

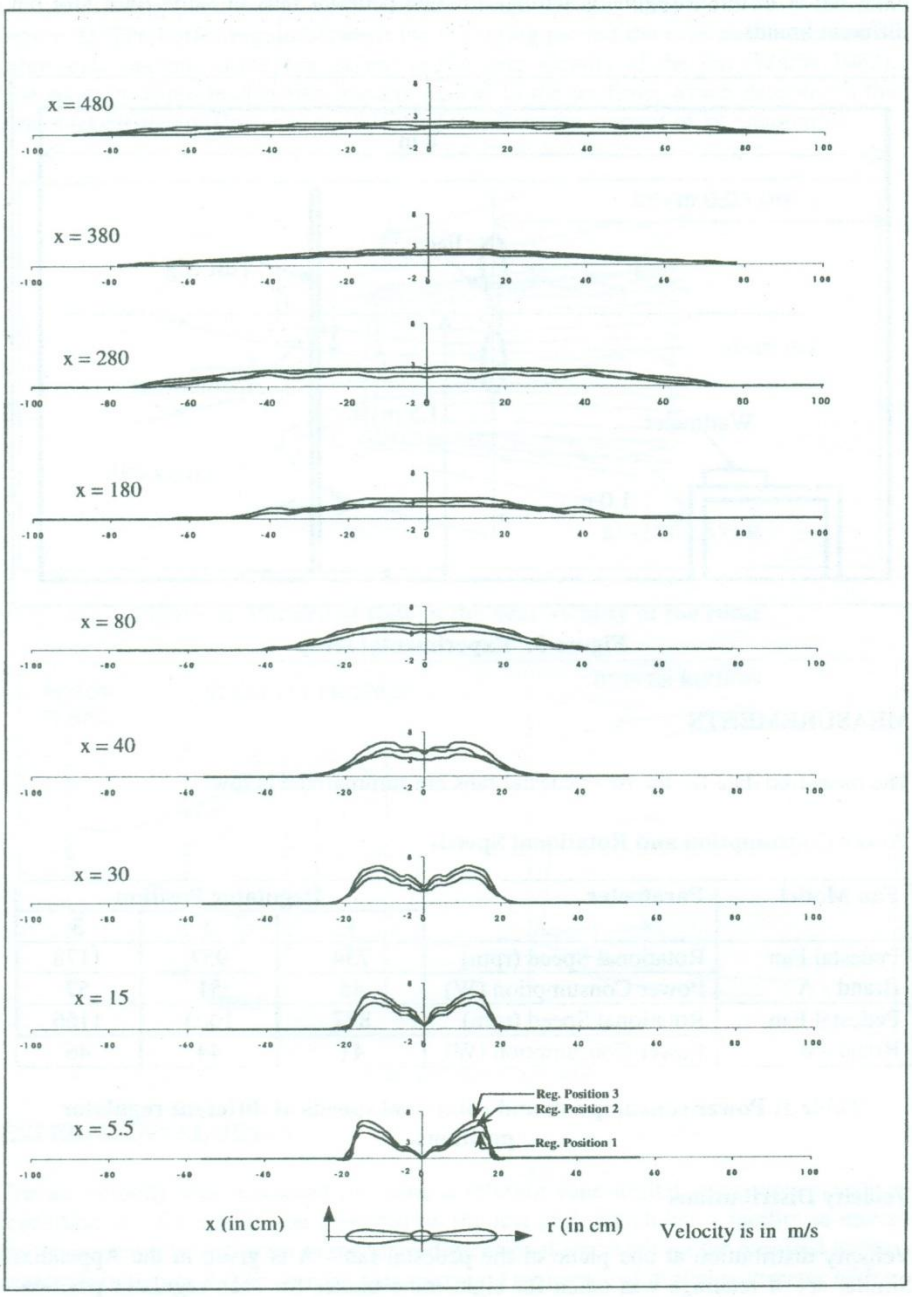

Figure 4: Axial velocity distribution generated by Fan-A at different regulator positions

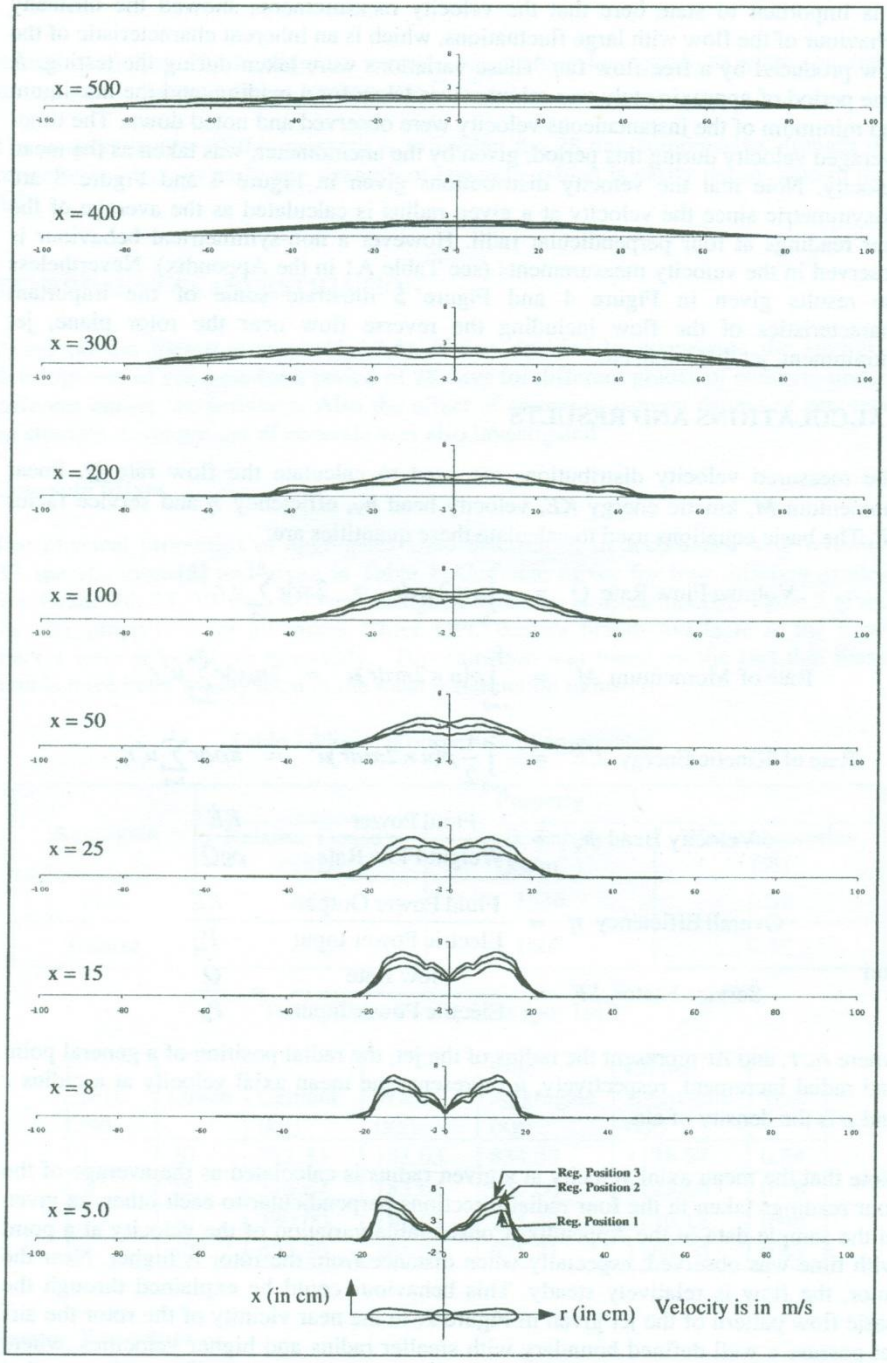

Figure 5: Axial velocity distribution generated by Fan-B at different regulator positions

It is important to state here that the velocity measurements showed the unsteady behaviour of the flow with large fluctuations, which is an inherent characteristic of the flow produced by a free-flow fan. These variations were taken during the testing. A time period of approximately two minutes was taken for a reading, and the maximum and minimum of the instantaneous velocity were observed and noted down. The time-averaged velocity during this period, given by the anemometer, was taken as the mean velocity. Note that the velocity distributions given in Figure 4 and Figure 5 are axisymmetric since the velocity at a given radius is calculated as the average of the four readings at four perpendicular radii. However a non-symmetrical behaviour is observed in the velocity measurements (see Table A1 in the Appendix). Nevertheless the results given in Figure 4 and Figure 5 illustrate some of the important characteristics of the flow including the reverse flow near the rotor plane, jet entrainment, jet diffusion, etc.

CALCULATIONS AND RESULTS

The measured velocity distributions are used to calculate the flow rate Q, linear momentum M, kinetic energy KE, velocity head h_V, efficiency η and service factor SF. The basic equations used to calculate these quantities are:

$$\text{Volume Flow Rate } \dot{Q} = \int_{r=0}^{r_o} u \times 2\pi r dr = 2\pi \Delta r \sum_{i=1}^{n} u_i r_i$$

$$\text{Rate of Momentum } \dot{M} = \int_{r=0}^{r_o} \rho (u \times 2\pi r dr) u = 2\pi \rho \Delta r \sum_{i=1}^{n} u_i^2 r_i$$

$$\text{Rate of Kinetic Energy } K\dot{E} = \int_{r=0}^{r_o} \frac{1}{2} \rho (u \times 2\pi r dr) u^2 = \pi \rho \Delta r \sum_{i=1}^{n} u_i^3 r_i$$

$$\text{Velocity Head } h_v = \frac{\text{Fluid Power}}{\text{Weight Flow Rate}} = \frac{K\dot{E}}{\rho g \dot{Q}}$$

$$\text{Overall Efficiency } \eta = \frac{\text{Fluid Power Output}}{\text{Electric Power Input}} = \frac{K\dot{E}}{P_{in}}$$

and

$$\text{Service Factor } SF = \frac{\text{Flow Rate}}{\text{Electric Power Input}} = \frac{\dot{Q}}{P_{in}},$$

where r_0, r, and Δr represent the radius of the jet, the radial position of a general point and radial increment, respectively, u represents the mean axial velocity at a radius r and ρ is the density of air.

Note that the mean axial velocity at a given radius is calculated as the average of the four readings taken in the four radial directions perpendicular to each other, as given in the sample data in the Appendix. Considerable variation of the velocity at a point with time was observed, especially when distance from the rotor is higher. Near the rotor, the flow is relatively steady. This behaviour could be explained through the basic flow pattern of the jet given in Figure 2. In the near vicinity of the rotor the air-jet possess a well defined boundary with smaller radius and higher velocities, where the buffer layer is limited to very thin layer. In this region, the flow is well controlled by the momentum of the jet imparted by the rotor. However, on the planes further away from the rotor the jet expands, flow rate increases, mean velocity decreases and

the buffer layer developed to a thicker regime. As the momentum of the jet becomes much smaller, the jet gets more susceptible to external disturbances and therefore becomes unsteady. These fluctuations are usually governed by the size of the room and the furniture and other solid boundaries present in the room.

The calculated results are presented in Table 2, Table 3, Table 4 and Table 5. The variations of the basic flow parameters along the air-jet of the two fans are given in Table 2 and Table 3.

Fan Type	Parameter	Regulator Position	Axial Distance (in number of rotor diameters)								
			0.14	0.38	0.75	1.00	2.00	4.50	7.00	9.50	12.00
Type - A	Flow Rate (m^3/s)	1	0.35	0.37	0.41	0.44	0.66	0.84	1.43	1.13	1.09
		2	0.39	0.49	0.52	0.57	0.96	0.89	2.09	1.47	1.91
		3	0.48	0.55	0.61	0.68	1.12	1.34	2.68	1.82	2.68
	Rate of Momentum (N)	1	1.50	1.59	1.72	1.45	1.83	1.43	2.00	1.23	0.94
		2	2.21	2.62	2.73	2.24	3.36	1.72	3.75	1.98	2.25
		3	3.10	3.33	3.75	3.54	4.44	3.44	5.84	3.08	3.83
	Rate of Kinetic Energy (W)	1	2.85	3.11	3.27	2.27	2.46	1.17	1.28	0.66	0.36
		2	5.41	6.45	6.52	4.42	5.84	1.69	3.16	1.33	1.22
		3	8.91	9.29	10.42	8.95	8.75	4.37	5.79	2.57	2.58
	Velocity Head (m)	1	0.69	0.72	0.67	0.44	0.32	0.12	0.08	0.05	0.03
		2	1.17	1.11	1.06	0.66	0.52	0.16	0.13	0.08	0.05
		3	1.57	1.44	1.45	1.12	0.67	0.28	0.18	0.12	0.08

Table 2: Variations of the flow parameters along the air-jet of Fan A.

Fan Type	Parameter	Regulator Position	Axial Distance (in number of rotor diameters)							
			0.20	0.38	0.63	1.25	2.50	5.00	7.50	10.00
Type - B	Flow Rate (m^3/s)	1	0.27	0.33	0.34	0.30	0.26	0.36	0.30	0.22
		2	0.32	0.36	0.38	0.33	0.31	0.42	0.39	0.31
		3	0.29	0.39	0.43	0.38	0.35	0.48	0.44	0.36
	Rate of Momentum (N)	1	1.18	1.30	1.27	0.62	0.24	0.26	0.16	0.06
		2	1.54	1.58	1.56	0.75	0.31	0.35	0.24	0.12
		3	1.32	1.89	1.98	0.93	0.39	0.41	0.31	0.14
	Rate of Kinetic Energy (W)	1	2.30	2.48	2.31	0.59	0.11	0.09	0.04	0.01
		2	3.42	3.32	3.06	0.79	0.15	0.13	0.07	0.02
		3	2.77	4.37	4.38	1.06	0.20	0.16	0.10	0.03
	Velocity Head (m)	1	0.71	0.64	0.58	0.17	0.04	0.02	0.01	0.00
		2	0.91	0.79	0.68	0.20	0.04	0.03	0.02	0.01
		3	0.80	0.95	0.86	0.24	0.05	0.03	0.02	0.01

Table 3: Variations of the flow parameters along the air-jet of Fan B.

The graphical representations of these variations are given in Figure 6 to Figure 13. The flow rate variation generated by Fan-A given in Figure 6 shows a continuous increase illustrating the jet entrainment process due to viscous shear. Flow rate becomes a maximum of about 4 to 6 times the flow rate near the rotor at about a distance of 7 rotor diameters downstream. Then further downstream the flow rate tends to decrease as a result of turbulent diffusion. The characteristic of the jet generated by Fan-B shows much inferior performance than that of Fan-A as the jet entrainment appears to be much weaker (see Figure 7). The jet entrainment

predominantly takes place up to about 0.6 rotor diameters downstream, where the flow rates become approximately 20 - 50% higher than that of at the rotor. Then the jet entrainment as well as diffusion takes place resulting fluctuating characteristics. The flow rates again reach a maximum at about 5 rotor diameters downstream, where the flow rates are approximately 30 - 60% higher than that near the rotor. Further downstream, jet diffusion becomes predominant and there is a continuos decrease in the flow rates. Note that there are large fluctuations in the flow rates, especially on the planes far downstream from the rotor. On these planes, the thickness of the buffer layer is considerably higher, where the flow velocity shows considerable fluctuations and therefore difficult to measure. As the flow rate in this regime can be considerable due to larger flow area, the calculated flow rates (as well as momentum) can exhibit large fluctuations.

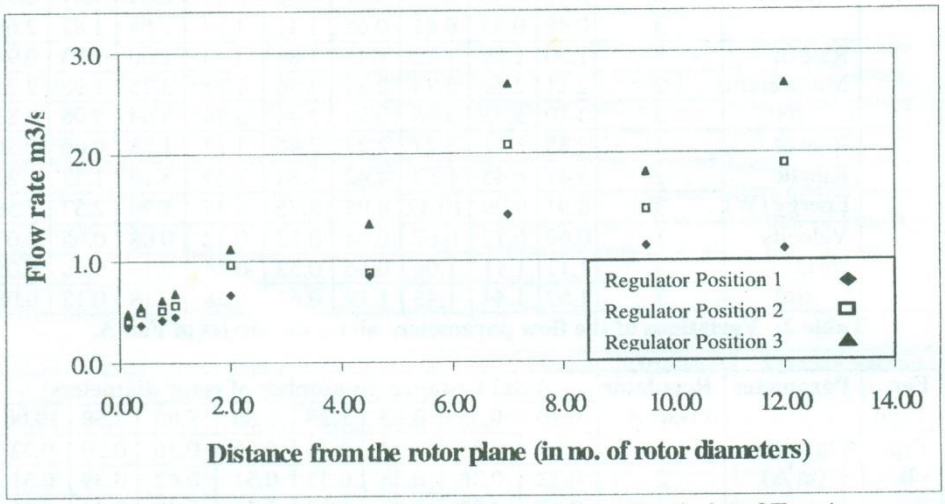

Figure 6: Variation of the volume flow rate along the air-jet of Fan-A.

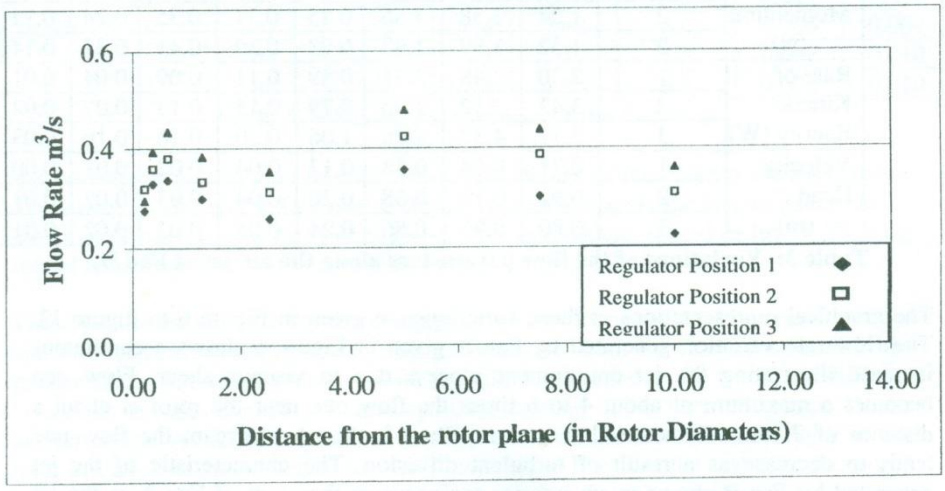

Figure 7: Variation of the volume flow rate along the air-jet of Fan-B.

The difference between the above characteristics of the two fans is difficult to explain with the existing data. One possible reason could be the level of swirl generated by the fan torque. A jet with a higher swirl diffuses more rapidly than that with a lower swirl component (Rajaratnam 1976). Another possibility is that the Fan-B generates higher turbulence level resulting higher rate of diffusion. In order to have a better understanding about these behaviors, the variations of the axial momentum of the jet of the two fans are plotted in Figure 8 and Figure 9.

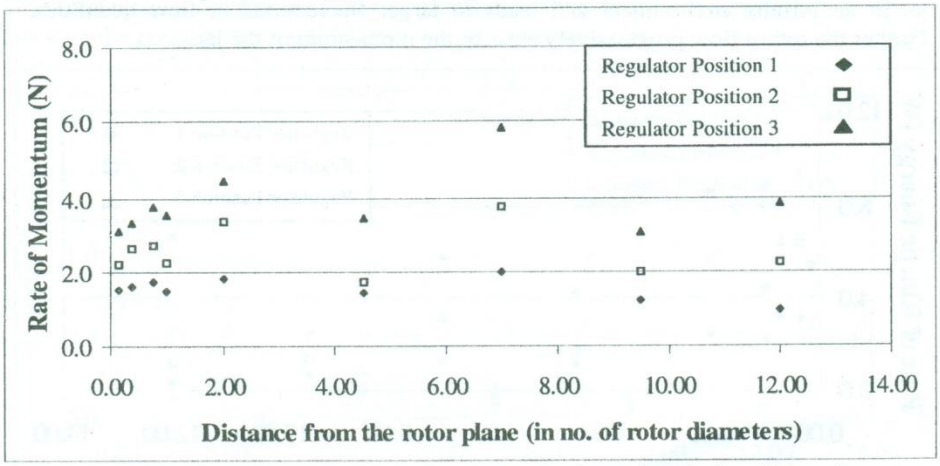

Figure 8: Variation of the rate of momentum along the air-jet of Fan-A

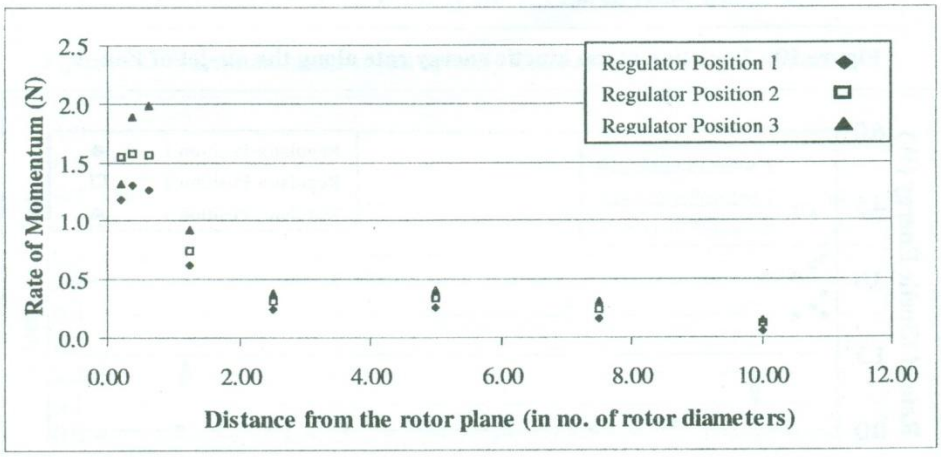

Figure 9: Variation of the rate of momentum along the air-jet of Fan-B

Both figures show a continuous increase in the axial momentum up to about a distance less than one rotor diameter. Axial momentum of Fan-B decreases rapidly indicating a strong diffusion of the jet, while that of Fan-A fluctuates but shows a slight decrease in trend indicating a higher penetrating capacity. The initial increase in the axial momentum of the jet is obvious because, as the jet converges, the pressure generated by the fan is converted into axial momentum. The resultant momentum reaches a maximum at the section with a minimum jet diameter. Therefore it could be concluded that the minimum jet diameter occurs at a distance less than one rotor

diameter (according to the present results, 0.75 diameters for Fan-A and 0.6 diameters for Fan-B). This is more apparent according to the variation of the kinetic energy (based on the axial velocity), as given in Figure 10 and Figure 11. It is important to state here that the jet flow generated by the fans is not an ideal jet in the sense that it is in a finite environment. For such confined flows, conservation of mass demands that a return flow be set up between the jet and the outer boundaries, which increases with the downstream distance. This behaviour results in a thicker buffer layer than that of a jet in an infinite environment and leads to larger fluctuations in flow quantities. Further the return flow progressively absorbs the momentum of the jet.

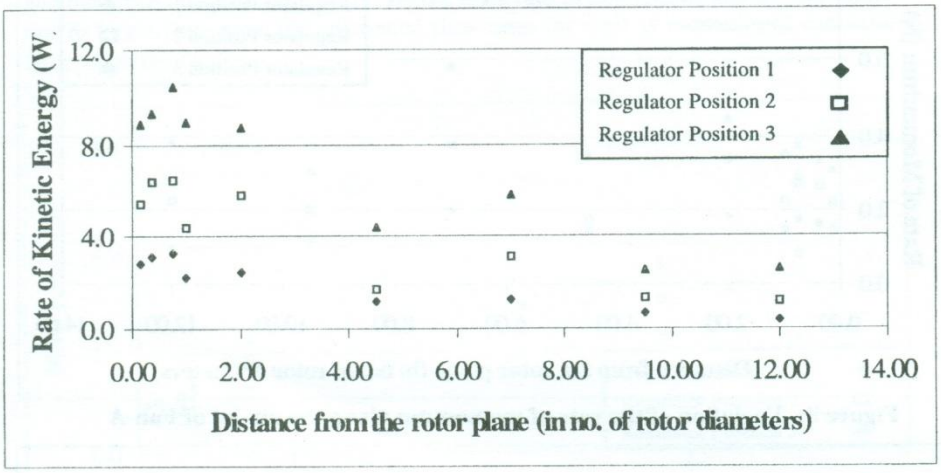

Figure 10: Variation of the kinetic energy rate along the air-jet of Fan-A

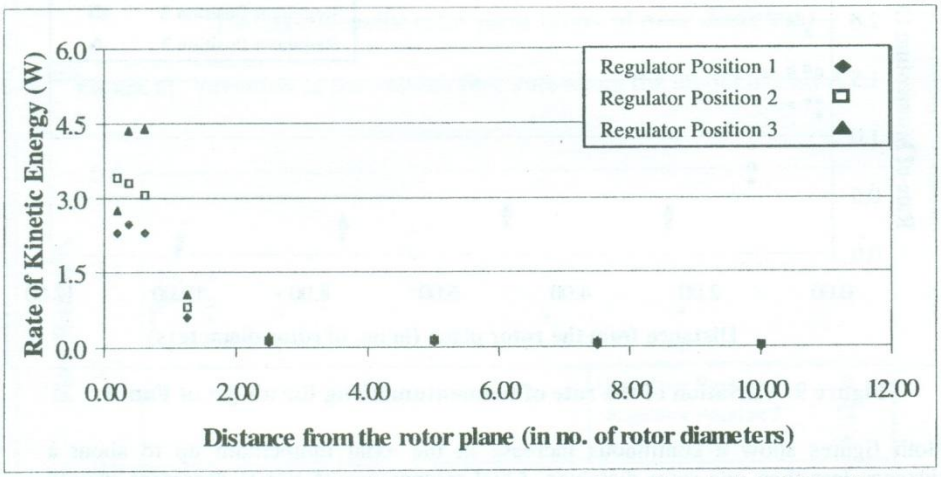

Figure 11: Variation of the kinetic energy rate along the air-jet of Fan-B

In both fans, the total rate of kinetic energy of the jet increases due to conversion of pressure energy to kinetic energy till the minimum jet diameter is reached, where the pressure energy becomes zero. Further downstream the kinetic energy of the jet decreases rapidly due to jet diffusion. The rate of diffusion is much higher for Fan-B

than that of Fan-A resulting in lower performance. The relative effects of the jet diffusion and pressure energy to kinetic energy conversion could be analyzed by evaluating a mean value for the velocity head of the fluid.

In the case of Fan-A, the mean velocity head remains approximately constant in the near vicinity of the rotor, where the pressure energy to kinetic energy conversion takes place. Therefore it could be concluded that this conversion rate is of the same order as the rate of jet diffusion. While the results of Fan-B indicate a higher diffusion rate than the pressure energy to kinetic energy conversion rate.

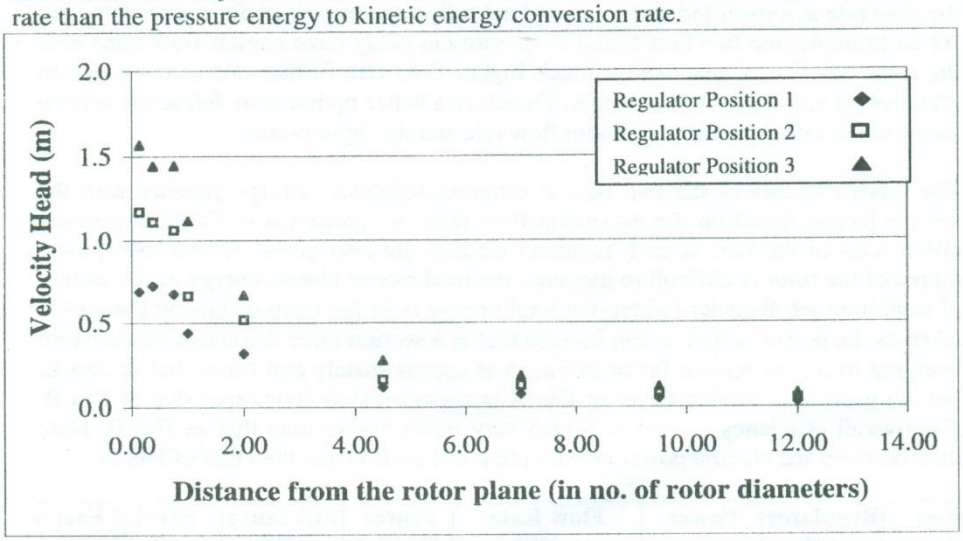

Figure 12: Variation of the mean velocity head along the air-jet of Fan-A

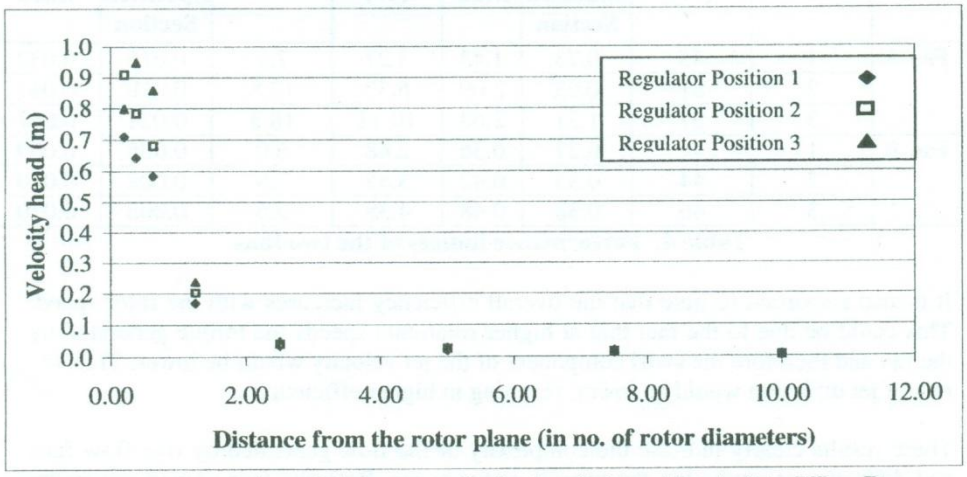

Figure 13: Variation of the mean velocity head along the air-jet of Fan-B

One of the prime objective of the present study is to identify a performance index to represent the overall performance of a given free-flow fan. The most commonly used parameter in fluid machinery is the overall efficiency, that is the output power to input power ratio. However for free-flow fans this quantity is difficult to predict as the output energy of the air (which includes both the pressure energy and the kinetic

energy) is difficult to measure. Further the energy of the fluid is in little use for the customer, what is important is the flow velocity generated by the fan. Therefore another performance index is defined for air-circulating fans, so called service factor, which is the ratio between the flow rate at a specified section from the rotor plane (three rotor diameters in the case of pedestal and table fans) to the electric power input to the fan (SLS 814 - Part 1). However, no specific values for the service factor have been defined to identify whether the performance of a given fan is satisfactory or not. Another disadvantage of the use of service factor as a performance index is that the flow rate at a specified section would not reflect the overall performance of the jet. As an example, the two fans tested in the present study have similar flow rates near the rotor but Fan-A generated a much higher flow rate further downstream due to effective jet entrainment than Fan-B. Therefore a better option is to define the service factor as the ratio between maximum flow rate and the input power.

The service factors of the two fans at different regulator settings together with the service factors based on the maximum flow rates are presented in Table 4. Further, efficiencies of the fans at each regulator settings are also given. As the total power output of the rotor is difficult to measure, the total rate of kinetic energy at the section of minimum jet diameter (where the total energy is in the form of kinetic energy) is taken as the power output. It can be seen that at a section three diameters downstream from the rotor, the service factor of Fan-A is approximately two times that of Fan-B, but the maximum service factor of Fan-A is approximately four times that of Fan-B. The overall efficiency of Fan-A is also very much higher than that of Fan-B. Note that, however the electric power consumption of Fan-B is less than that of Fan-A.

Fan Type	Regulator Position	Power Consump. (W)	Flow Rate (m^3/s)		Power Output (W)	Efficiency (%)	Service Factor ($m^3/s/W$)	
			Specified Section	Max			Specified Section	Max.
Fan-A	1	45	0.73	1.43	3.27	7.3	0.016	0.032
	2	51	0.93	2.09	6.52	12.8	0.018	0.041
	3	57	1.21	2.68	10.42	18.3	0.021	0.047
Fan-B	1	41	0.27	0.36	2.48	6.0	0.006	0.009
	2	44	0.33	0.42	3.42	7.8	0.008	0.010
	3	46	0.38	0.48	4.38	9.5	0.008	0.010

Table 4: Performance indices of the two fans

It is also important to note that the overall efficiency increases with the rotor speed. This could be due to the fact that at higher rotational speeds the torque generated by the fan and therefore the swirl component of the jet velocity would be lower. Thus the rate of jet diffusion would be lower, resulting in higher efficiencies.

These results clearly indicate the complexity of the flow generated by free-flow fans and difficulty of predicting the overall performance. Both the fans considered in the present study generated a similar axial velocity distribution at the rotor, but different behaviour of the overall jet developments leading to a vast difference in the performances. As an example, the velocity distributions at the near vicinity of the rotor of Fan-A at the regulator position 2 and that of Fan-B at the regulator position 3 are plotted in Figure 14. It can be seen that the two velocity distributions are quite similar, resulting volume flow rates of 0.392 m^3/s and 0.394 m^3/s, respectively.

However, as shown in Figure 15 the jet development behaviour of the two cases are not similar; one jet shows a strong entrainment with considerable increase in the flow rate in downstream direction, while the other jet shows very little increase in the flow rate indicating higher diffusion.

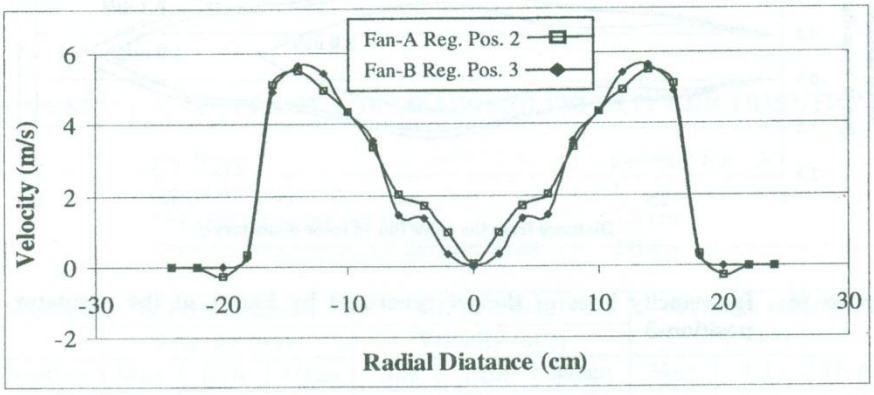

Figure 14: Velocity profiles at the near vicinity of the rotors of the two fans

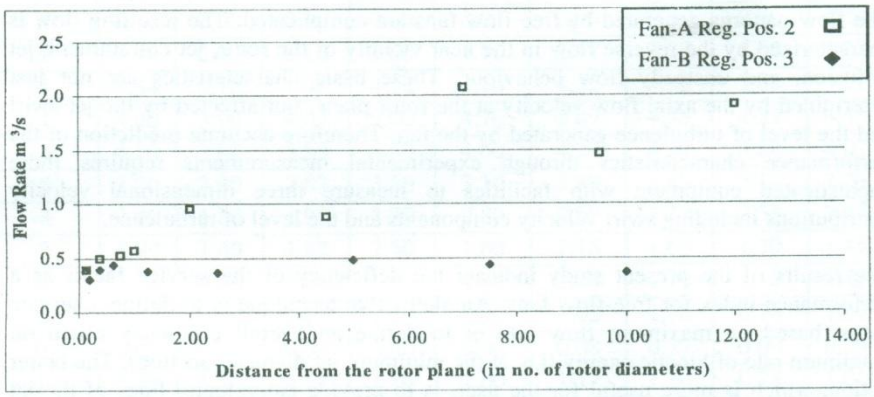

Figure 15: Comparison of the jet development behaviours of the two fans

The above results also indicate the limitations of the service factor as a performance index for free-flow fans. However, both the overall efficiency based on the rate of kinetic energy at the minimum jet diameter section and the service factor based on the maximum flow rate illustrate clearly the relative performances of the two fans. Therefore, these two indices would be more appropriate for performance evaluation of free-flow fans.

Further, as free-flow fans are widely used for air circulation and comfort, it would be more appropriate to define a comfort region that a fan could cover at each regulator setting. This is achieved by forming iso-velocity lines based on the axial velocity distribution generated by a given fan. As an example, iso-velocity lines for Fan-A at the regulator position 3 are illustrated in Figure 16.

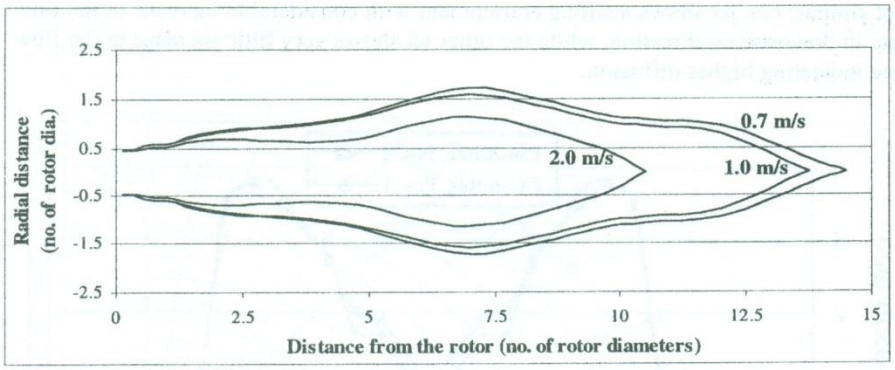

Figure 16: Iso-velocity lines of the jet generated by Fan-A at the regulator position-3

CONCLUSIONS

The flow patterns generated by free-flow fans are complicated. The resulting flow is characterized by the reverse flow in the near vicinity of the rotor, jet entrainment, jet diffusion, and unsteady flow behaviour. These basic characteristics are not just determined by the axial flow velocity at the rotor plane, but affected by the jet swirl and the level of turbulence generated by the fan. Therefore accurate prediction of the performance characteristics through experimental measurements requires more sophisticated equipment with facilities to measure three dimensional velocity distributions including swirl velocity components and the level of turbulence.

The results of the present study indicate the deficiency of the service factor as a performance index for free-flow fans. An alternative technique is to define a service factor based on maximum flow rate or to define an overall efficiency based on maximum rate of kinetic energy (i.e. at the minimum jet diameter section). The better option, which is more useful for the user, is to provide iso-velocity lines of the jet generated by the fan at each regulator setting together with the power consumption by the fan.

REFERENCES

AHMAD, J. & DUQUE, E.P.N. 1996. Helicopter rotor blade computation in unsteady flows using moving embedded grids. J. Aircraft, 33, pp. 54-60.

CONLISK, A.T. 1997. Modern Helicopter Aerodynamics. Ann. Rev. Fluid Mech., 29, pp. 515-567.

RAJARATNAM, N, 1976. Turbulent jets. Elsevier Scientific Publishing Company.

SLS 814 - Part 1. SRI LANKA STANDARD, Specification for electric fans and regulators - Part 1 - Performance.

SUGATHAPALA, A.G.T. 1997. Performance analysis of free-flow fans: A theoretical and experimental study. Seminar on Contribution to the Energy Scenario in Sri Lanka, SLAAS, Colombo 07, Sri Lanka, 26th November 1997 (unpublished).

WALLIS, R.A. 1983. Axial flow fans and ducts. John Wiley & Sons Inc.

APPENDIX: A SAMPLE OF THE MEASURED VELOCITY DISTRIBUTION

Fan Type : Pedestal fan - A
Regulator Position : 1
Distance from the fan rotor : 5.5 cm
Distance between two radial positions : 2.0 cm

Direction	AB (Horizantal)			CD (Vertical)			Average velocity (m/s)		
	Velocity (m/s)			Velocity (m/s)					
Position	Max	Min	Mean	Max	Min	Mean	Max	Min	Mean
-12	0.00	0.00	0.00	0.00	0.00	0.00	0.00	0.00	0.00
-11	0.00	0.00	0.00	0.00	0.00	0.00	0.00	0.00	0.00
-10	0.00	0.00	0.00	0.00	0.00	0.00	-0.20	0.00	-0.04
-9	0.50	0.00	0.10	2.60	1.70	2.17	2.15	1.68	1.87
-8	1.44	0.70	1.04	4.70	4.10	4.32	4.33	3.83	4.11
-7	4.40	3.90	4.05	5.00	4.70	4.89	4.58	4.35	4.45
-6	4.10	3.80	3.89	4.50	4.00	4.29	4.20	3.88	4.02
-5	3.20	2.80	2.82	3.50	3.10	3.39	3.48	3.18	3.29
-4	2.20	1.80	1.96	3.30	2.80	2.99	2.83	2.55	2.67
-3	1.90	1.40	1.82	2.50	1.80	2.16	1.65	1.30	1.48
-2	1.40	0.10	1.06	1.50	1.10	1.25	1.70	1.10	1.45
-1	0.80	0.00	0.61	1.10	0.90	1.02	1.10	0.78	1.01
0	0.04	0.00	0.09	0.50	0.00	0.08	0.27	0.00	0.09
1	1.40	1.20	1.22	1.10	1.00	1.17	1.10	0.78	1.01
2	1.60	1.40	1.43	2.30	1.80	2.06	1.70	1.10	1.45
3	1.60	1.50	1.35	3.10	2.80	2.92	1.65	1.30	1.48
4	2.20	2.10	2.18	3.60	3.50	3.55	2.83	2.55	2.67
5	2.90	2.70	2.76	4.30	4.10	4.20	3.48	3.18	3.29
6	3.60	3.20	3.36	4.60	4.50	4.53	4.20	3.88	4.02
7	4.10	4.00	4.04	4.80	4.80	4.80	4.58	4.35	4.45
8	4.40	4.30	4.44	3.90	3.10	3.57	4.33	3.83	4.11
9	4.90	4.50	4.67	0.60	0.50	0.55	2.15	1.68	1.87
10	-0.40	0.00	-0.14	-0.40	0.00	-0.01	-0.20	0.00	-0.04
11	0.00	0.00	0.00	0.00	0.00	0.00	0.00	0.00	0.00
12	0.00	0.00	0.00	0.00	0.00	0.00	0.00	0.00	0.00

Table A1: Axial velocity distribution of the jet at different planes from the rotor